Ab Initio Investigation of the Hydrogen Interaction on Two Dimensional Silicon Carbide

Phi Minh Nguyen, Hoa Van Nguyen, Vi Toan Lam, Tranh Thi Nhu Duong, Tet Vui Chong, and Hanh Thi Thu Tran*

Read Online

ACCESS | Metrics & More | Article Recommendations

ABSTRACT: A series of density functional theory calculations were performed to understand the bonding and interaction of hydrogen adsorption on two-dimensional silicon carbide obtained from molecular dynamics simulation. The converged energy results pointed out that the H atom can sufficiently bond to 2D SiC at the top sites (atop Si and C), of which the most stable adsorption site is T_{Si}. The vibrational properties along with the zero-point energy were incorporated into the energy calculations to further understand the phonon effect of the adsorbed H. Most of the 2D SiC structure deformations caused by the H atoms were found at the adsorbent atom along the vertical axis. For the first time, five SiC defect formations, including the quadrilateral-octagon linear defect (8-4), the silicon interstitial defect, the divacancy (4-10-4) defect, the divacancy (8-4-4-8) defect, and the divacancy (4-8-8-4) defect, were investigated and compared with previous 2D defect studies. The linear defect (8-4) has the lowest formation energy and is most likely to be formed for SiC materials. Furthermore, hydrogen atoms adsorb more readily on the defect surface than on the pristine SiC surface.

Five different defects in 2D SiC
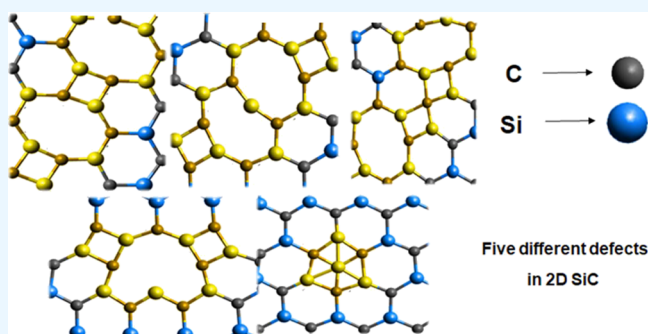
1. INTRODUCTION

Since 2004, after the discovery of graphene, two-dimensional (2D) thin hexagonal forms of materials have increasingly attracted attention.[1−6] Research has been done on group IV elements, not only on the special element C, but also on other elements such as Si, Ge, Sn, and Pb. Khan et al. showed that, for the silicon element, it is very complicated to construct a stable structure of nanotubes or graphene-like sheets.[7] However, the silicene (the mixture of Si) on the silver substrates was synthesized by Aufray et al. and Vogt et al.[8,9] In addition, by using an experimental method such as high-temperature thermochemical Si powder reactions, the quasi-2D SiC flake was created.[10]

Previous theoretical studies have shown that the 2D SiC has a planar structure like graphene but with a longer bond length (1.77−1.85 Å) and a larger bandgap (2.5−2.6 eV).[6,11,12] As a large bandgap semiconductor, SiC materials are predicted to have large applications for nanodevices operating under high temperature, and high-frequency conditions.[13] Recently, many theoretical research groups have continued to focus on studying the configurations and characteristics of 2D SiC models by using molecular dynamics (MD) and density functional theory (DFT) simulation methods.[3,4,14−16] However, these theoretical studies give SiC models with different bond length values, leading to varying properties of 2D SiC

models. For example, Sun's group found a SiC length of ~1.77 Å,[3] while Susi's group showed that the bond length between the Si and C atoms in the model is ~1.89 Å.[6] Moreover, with the 2D silicon carbide models obtained from previous studies, there are existing defects that have not been studied in detail.[3,4,6] Therefore, in this study, we study the 2D SiC model in detail by combining MD and DFT methods. Furthermore, based on the obtained accurate and convincing 2D SiC model, we continued to conduct a series of DFT calculations to determine the hydrogen adsorption properties of 2D SiC in this study. The convergence control and the zero-point vibrational effect have been carefully calculated in the study.

In Section 3.1, the adsorption sites and the adsorption energies were precisely investigated by considering the zero-point vibrational effect. Several hydrogenated 2D SiC configurations have been simulated to understand the most favorable adsorption site for hydrogen atoms. The possible structure deformations of 2D SiC caused by the adsorbed

hydrogen atoms are also noted and investigated. For the first time, five different defect types of the 2D SiC model were explored and discussed in Section 3.2. These defects are the quadrilateral-octagon linear defect (8-4), the silicon interstitial defect, the divacancy (4-10-4) defect, the divacancy (8-4-4-8) defect, and the divacancy (4-8-8-4) defect.

2. CALCULATION

2.1. Large-Scale Atomic/Molecular Massively Parallel Simulator Simulation. To construct the 2D SiC model, the software package LAMMPS (large-scale atomic/molecular massively parallel simulator) was used. LAMMPS is a classical molecular dynamics code with a focus on materials modeling.[17] The crystalline 2D SiC model of the honeycomb structure with 6240 atoms was created. The Si−C bond length of 1.787 $\mathring{A}$ was set up.[3] First, the model was relaxed at 300 K for 3×10^5 MD steps using the *NPT* ensemble. The periodic boundary conditions with Vashishta potential were used.[18] Then, the model applied the elastic reflection boundary along the *y*-axis and retained the periodic boundary condition along the *x*-axis to get the armchair SiC nanoribbon. After that, the obtained SiC nanoribbon was relaxed at a temperature of 300 K for 2×10^5 MD steps. In the next step, the relaxed SiC nanoribbon was heated up to 8000 K at the heating rate of 10^{11} K/s to get a complete liquid state. Then, the obtained model was relaxed at a temperature of 8000 K for 3×10^5 MD steps. To obtain the crystal structure, the liquid SiC model was rapidly cooled down to 300 K at a cooling rate of 10^{13} K/s. After relaxing at 300 K for 3×10^5 MD steps, the relaxed structure of the solid SiC model has bond lengths between the Si and C of ~1.85 $\mathring{A}$. This bond length is much larger than that in other studies of 1.77−1.79 $\mathring{A}$,[3,19] but it is closer to 1.89 $\mathring{A}$ as reported.[6,20] The model has no buckling, as expected from the sp² hybridization type.[3,19]

2.2. Spanish Initiative for Electronic Simulations with Thousands of Atoms Simulation. We used the DFT method implemented in the SIESTA (Spanish Initiative for Electronic Simulations with Thousands of Atoms) package, which is the combination of self-consistent field loop, norm-conserving pseudopotential, and plane-wave basis set, to calculate the ground-state energies and the optimized structures of all the simulation models.[21−23] For the exchange and correlation energy functional, we applied the generalized gradient approximation, in the form of a revised Perdew−Burke−Ernzerhof functional.[24,25] We also employed the double-zeta polarized basis sets, while using the energy cutoff of 200 Ry for all the simulations. The structural relaxations were performed under the two-dimensional periodic boundary condition while using the vacuum gap of 40 $\mathring{A}$ in the *z*-axis to neglect most of the interaction between the periodic lateral layers. The geometry optimization loop is stopped when the maximum stress component is less than 0.02 eV $\mathring{A}^{-1}$. In the previous DFT calculations, those selected parameters have provided reasonable accuracy.[2,26−29]

For long-range interactions of adsorbed hydrogen atoms, it is important to calculate the bond lengths and energies of the hydrogen molecules correctly. Hence, the extended basic set was added to calculate the adsorbed hydrogen atoms in this study. The energy shift of 60 meV and the split norm of 0.53 for the second zeta were used for H atoms. The obtained H_2 bond length is 0.75 $\mathring{A}$, which is in good agreement with the experiment of 0.74 $\mathring{A}$.[30] The binding energy and the zero-point energy (ZPE) are calculated as 4.52 and 0.27 eV, respectively.

Those values are in good agreement with the experimental results of Landau and Lifshitz in 1958 (4.53 and 0.27 eV, respectively).[31] The calculated values of the rotational free energy and the translational free energy of the H_2 molecule are −0.04 and −0.30 eV, respectively. The total energy of one hydrogen atom obtained from the simulation is −13.54 eV, which is in good agreement with Landau's experiment of −13.6 eV.[31]

At first, a periodic (7×7) supercell SiC monolayer, consisting of 49 silicon atoms and 49 carbon atoms (see Figure 1), was cut out from the obtained MD simulated structure. We
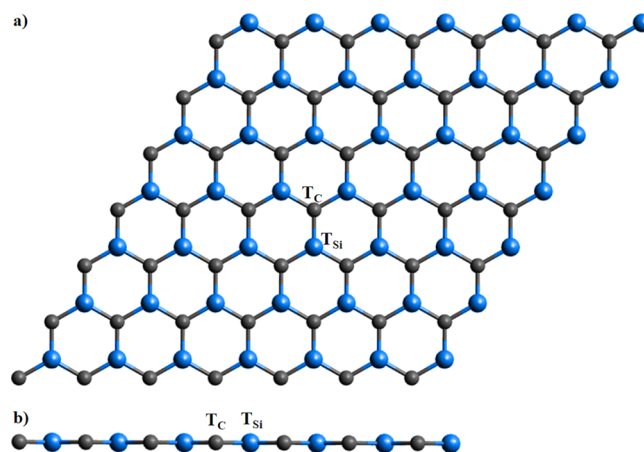

Figure 1. Top view (a) and nonbuckling side view (b) of the two-dimensional silicon carbide model include a total of 98 atoms, where T_C and T_{Si} sites are atop C (gray ball) and Si (blue ball) atoms, respectively.

decided to choose a (7×7) supercell because the size effect is negligible when the size is larger than a (4×4) supercell.[32] To test on the adsorption site, a hydrogen atom was put atop the SiC sheet at the possible sites. After that, we check the converged data regarding the increasing *k*-point grid from the $(1 \times 1 \times 1)$ to $(13 \times 13 \times 1)$ Monkhorst−Pack scheme (MP). Zero-point vibrational energy is also considered for better results.

2.3. ZPE and Defect Calculations. Due to the hydrogen vibrations around the equilibrium position significantly affecting the interaction energy of the adsorption system, the vibrational effect is taken into account for the calculation of hydrogen adsorption energy.[33,34] In this work, the vibrational energy of adsorbed H atoms on the SiC surface, which is called the hydrogen ZPE, was calculated using the following equation:

$$\text{ZPE} = \frac{h}{4\pi} \sqrt{\frac{k(m_1 + m_2)}{m_1 m_2}}$$

where m_1 is the hydrogen mass, m_2 is the Si/C mass, h is Planck's constant, and k is the force constant. Force constant k can be calculated by using the least squares calculation method when the H atoms are displaced around the obtained equilibrium sites in both the normal and parallel directions.

To study the 2D SiC defects, the model of 98 atoms (49 Si atoms and 49 C atoms) is taken into account. Five defects are found, namely, the quadrilateral-octagon linear defect (8-4), the silicon interstitial defect, the divacancy (4-8-8-4) defect, the divacancy (8-4-4-8) defect, and the divacancy (4-10-4) defect. The defect formation energy (E_{form}) is calculated by

subtracting the total energy of the defective model (E_{defect}) from the total energy of the nondefective model ($E_{non\text{-}defect}$):

$$E_{form} = E_{non-defect} - E_{defect}$$

3. RESULTS AND DISCUSSIONS

3.1. Hydrogen Possible Adsorption Sites. To test the possible adsorption site, the hydrogen atoms were put on the relaxed SiC sheet on the high symmetry possible adsorption sites: Top C (T_C), Top Si (T_{Si}), Center (C), and Bridge (B). After the conjugate gradient steps between the self-consistent field cycles, the H atoms will be relaxed to nearby stable positions. The optimized system with the $(3 \times 3 \times 1)$ k-point shows that only the top sites (T_C, T_{Si}) are stable (see Figure 2). Similar results on the stable adsorption sites of hydrogen on
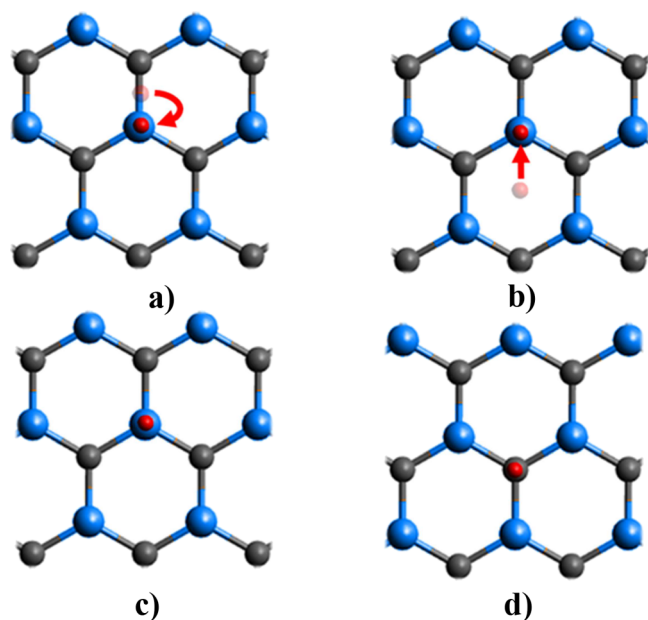

Figure 2. H atoms (red ball) on the bridge (a) and the center (b) sites are not stable and shift to the T_{si} site after optimization, while the T_{Si} (c) and T_C (d) sites are stable adsorption sites.

the surface of 2D materials have also been reported.[32] Because Si and C have an sp² hybridization proven by the planar 2D-SiC sheet, this leaves a half-occupied P_z orbital for both Si and C atoms (the P_z orbital is perpendicular to the 2D-SiC sheet). Hydrogen should be naturally attracted to this site to share the electron. Looking at Mulliken charge analysis results when comparing the charge transfer of the adsorbent atom before and after hydrogen adsorption, the most differences are at the s and P_z orbitals (see Table 1). The hydrogen adsorbed on 2D-SiC interacted mostly with the P_z orbital leading to the preferred adsorption sites being the Top sites.

Next, to determine the model's convergence results via increasing the k-point value, the adsorption energies of T_C and T_{Si} systems are calculated with different MP grids. It shows that the adsorption energy does not change when using the $(3 \times 3 \times 1)$ MP grid. Therefore, the k-point of $(3 \times 3 \times 1)$ MP grids was used for all the following systems. This is a rather low number of k-points but has been used before in larger cell 2D SiC DFT calculations.[6]

To calculate the hydrogen adsorption energy, the following equation was used:

Table 1. Mulliken Electron Charge Transfers of the Adsorbent Atoms before and after Hydrogen Adsorption

	Top Si			Top C		
	Si	Si with H	charge transfer	C	C with H	charge transfer
s	**1.036**	**0.920**	**0.116**	**1.013**	**0.911**	**0.102**
P_x	0.729	0.720	0.009	0.981	1.046	0.065
P_y	0.727	0.718	0.009	0.987	1.054	0.067
P_z	**0.691**	**0.769**	**0.078**	**1.063**	**0.928**	**0.135**

$$E_{ads} = E(n_H) - E(0) - \frac{n_H}{2}E_{H_2}$$

where E_{ads} is the hydrogen adsorption energy, $E(n_H)$ is the total energy of the H/SiC system with n_H hydrogen atoms, $E(0)$ is the total energy of bare 2D SiC, and E_{H_2} is the total energy of the isolated H_2 molecule. The adsorption energies of hydrogen on T_{Si} and T_C sites with the optimized Si/C−H bond lengths are shown in Table 2.

The distortion around the adsorption position is displayed in Figure 3. The distortion is not observed from the top view, which shows that there are small displacements in the in-plane axes. At the absorption site, the carbon atom is attracted up along the vertical axis more strongly than the Si atoms (z_C = 0.460 Å, z_{Si} = 0.369 Å), and the first neighboring Si atoms are also attracted upward of about 0.06 Å, forming local deformations around the adsorbent C atom at the H adsorption site (Figure 3a). Those local hill-forming properties were also noted in the previous study of graphene.[32] However, the displacements of the first neighbor C atoms around the adsorbent Si atom were not clearly observed (Figure 3b). It means that the Si atoms are more stable than the C atoms in the 2D SiC system, and this is well-agreed with the adsorption energies shown in Table 2.

The hydrogen vibrational effect, the ZPE, is shown in Table 3. Similar to the previous study on hydrogen adsorption,[28] strong fluctuation of hydrogen is observed along the z-axis, while the fluctuations along the x and y axes are very weak (Figure 4). Comparing the ZPE of H on the 3D Pt surface (~160 meV),[28] the vibrational effect of the hydrogen atom on the 2D surface is not significant. The finding of the vibrational ZPE's effect on the 2D silicon carbide system, which has not been reported to date, can provide the necessary information for further research on the interaction of hydrogen on the 2D SiC surface.

The free energy of the adsorbed hydrogen state in reference to hydrogen in the gas phase was calculated using the equation below

$$\Delta G_H = E_{ads} + \Delta E_{ZPE} - T\Delta S_H$$

where E_{ads} is the hydrogen adsorption energy. While ΔE_{ZPE} and ΔS_H are the ZPE difference and the entropy difference between the adsorbed state and the gas phase hydrogen, respectively. The E_{ads} and ΔE_{ZPE} are obtained from the adsorption energy and vibrational energy calculation above. For the entropy term, we observed that the adsorbed hydrogen on the 2D-SiC vibrates less than the hydrogen on the 3D Pt surface,[27,29] thus the vibrational entropy of hydrogen in the adsorbed state is small and neglectable.[39−41] The ΔS_H can be estimated as approximately $\frac{1}{2}S^0_{H_2}$, with the $S^0_{H_2}$ being hydrogen molecule entropy taken from the thermochemical tables at 298.15 K of temperature and 1 bar of pressure.[42]

Table 2. Bond Length of the Adsorbent Atom (Si and C Atoms) with the H Atom on Top of Itself (d_{a-H}, Å), the Distance of the Adsorbent Atom with Their Neighbors (d_{Si-C}, Å), the Vertical Displacement of the Adsorbent Atom Compared with Their Relaxed Positions (h, Å), and the Hydrogen Adsorption Energies (E_{ads}, eV)

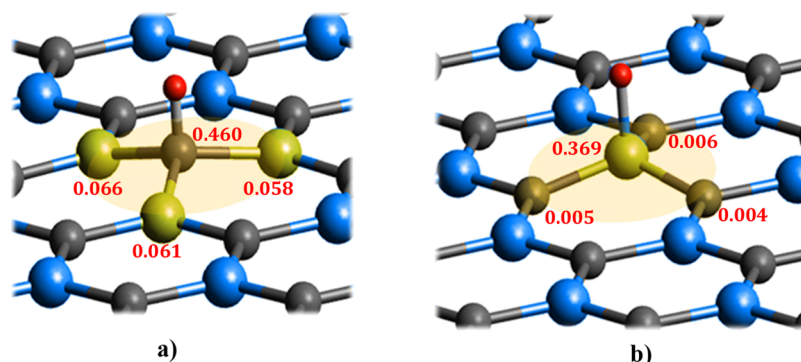| site	fixed 2D SiC				nonfixed 2D SiC			
	d_{a-H}	d_{Si-C}	h	E_{ads}	d_{a-H}	d_{Si-C}	h	E_{ads}
T_C	1.149	1.865	0	−0.374	1.117	1.975	0.460	−1.073
T_{Si}	1.580	1.865	0	−0.712	1.525	1.929	0.369	−1.244

Figure 3. Out-of-plane distortion at the neighbors of the adsorbent atom (highlighted atoms) in T_C (a) and T_{Si} (b) adsorption configurations. Displacements of the Si and C atoms along the z-axis (Å) are shown by the red numbers.

Table 3. Force Constants (k, eV/Å²), Vibrational Frequencies (f, cm⁻¹), ZPE (meV), and Free Energy of the Absorbed H (ΔG_H, eV)

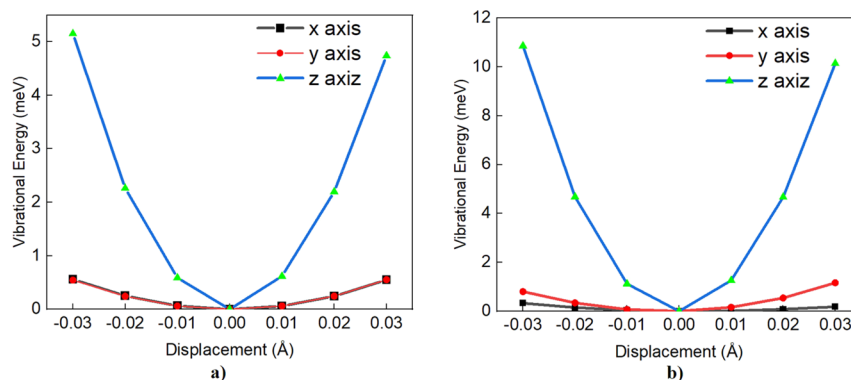|	Top C			Top Si		
	x-axis	y-axis	z-axis	x-axis	y-axis	z-axis
k (eV/Å²)	0.0357	0.135	1.454	0.0771	0.0756	0.681
f (cm⁻¹)	8.483	16.526	54.165	12.474	12.353	37.063
ZPE (meV)	0.526	1.02	3.36	0.773	0.766	2.30
total ZPE (meV)	4.91	3.84				
ΔG_H (eV)	−0.1669	−0.5059				

Figure 4. Vibrational energies of the adsorbed hydrogen on T_{Si} (a) and T_C (b) sites have good correspondence with the harmonic approximation.

The negative ΔG_H suggests the hydrogen-adsorbed reaction on 2D-SiC at the standard condition is a spontaneous and exothermic process. Although ΔG_H shows 2D-SiC to be not better than Pt as a hydrogen evolution reaction electrocatalyst, which usually requires $|\Delta G_H| \leq 0.1$ eV,[40] hydrogen can be stably adsorbed on the 2D-SiC surface at standard conditions, and the values of free energy in Table 3 again indicate that the adsorbed hydrogen at the Si site is much more stable than hydrogen at the C site.

3.2. Structural Defects of 2D Silicon Carbide. Five defects were found from the 2D SiC model obtained by the

MD simulation: the quadrilateral-octagon linear defect (8-4 defect), the silicon interstitial defect, and three other defects that appear in conjunction with the linear 8-4 defect, including the divacancy (4-8-8-4) defect, the divacancy (8-4-4-8) defect, and the divacancy (4-10-4) defect (see Figure 5).

Previous studies have shown that the nonmagnetic ground state is commonly observed, and the dangling bonds are rare to find in the system.[35] Similar results are also obtained in our study. Table 4 shows that the lowest formation energy is found for the quadrilateral-octagon linear defect. It means that, in the 2D SiC system, the 8-4 defect is the most stable and the most
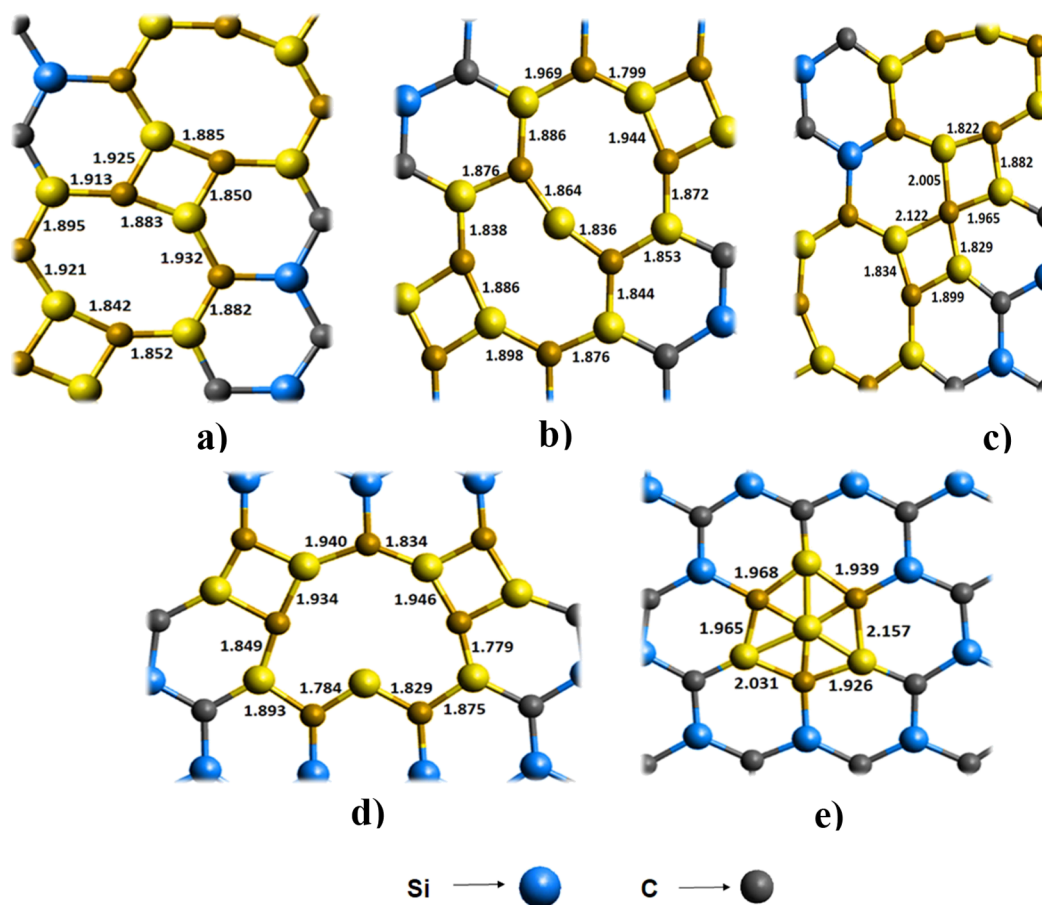
Figure 5. Structural defects (yellow highlight) in two-dimensional silicon carbide: (a) the linear (8-4) defect; (b) the divacancy (4-8-8-4) defect; (c) the divacancy (8-4-4-8) defect; (d) the divacancy (4-10-4) defect, and (e) the silicon interstitial defect.

Table 4. Formation Energy of the Defects in 2D SiC (eV)

structural defect	formation energy
linear (8-4) defect	7.60537
silicon interstitial defect	10.0246
divacancy (4-10-4)	12.7898
divacancy (8-4-4-8)	8.46357
divacancy (4-8-8-4)	9.51503

well-formed. Our result is contrary to the previous studies of Padilha,[35] who observed that the single vacancy defect is the most stable. The difference between our formation defects and Padilha's defects may be due to the buckled structure of germanene, which is not observed in silicon carbide. In addition, the larger value of the lattice constant and the smaller value of the in-plane nearest-neighbor distance also affect the formation of the defects.

There are three other variants of the 8-4 defect, which are the divacancy (4-8-8-4) defect, the divacancy (8-4-4-8) defect, and the divacancy (4-10-4) defect. All of them have higher formation energy than the original linear defect, while the divacancy (4-10-4) defect has the highest formation energy among all the defects, proving this defect is the most unlikely to form. These divacancy defects are found to appear at the end of the linear defect, but no single vacancy or triple vacancy defects are found. Because in 2D materials, the divacancy defects with an even number of absent atoms are usually more energetically stable compared to the single vacancy or triple vacancies. As the result of the optimized dangling bond,[36,37] we

also noted that most of the Si−C bondings in all the defects fluctuate between 1.8 and 2.0 Å and there is no buckling defects. The linear defect (8-4) in 2D SiC seems like the single-crystalline grains of repeated 4 and 8 Si and C atoms, that were created when two lattices have misorientation of about 30° coincide. This pattern of the linear defect was also found in other hexagonal structures including boronitrene and phosphorene,[36] but it is not a common pattern of linear defect found in most 2D hexagonal materials. The (5-7) pattern is a more common type of grain boundary defect. It was found in graphene, boronitrene, MoS_2, germanene, and phosphorene.[2,36] Other point-defect types, dislocations, and Stone−Wales defects, which are intensively studied in the previous 2D material,[35,18] are not found in this 2D SiC model. The interstitial defect, often seen in the bulk material, surprisingly appears in the 2D SiC material (Figure 5e). The Si atom appears in the middle of the hexagonal ring, causing the honeycomb structure to be divided into six triangular structures. The bondings of the Si interstitial atom with the hexagonal ring are about ∼2.2 Å (Si−Si) and ∼1.8 Å (Si−C), which are within the range of normal Si−Si bonds (2.358 Å)[38] and Si−C bond in this paper (∼1.865 Å). This defect is due to the bigger rings of the 2D SiC (Si−C ∼ 1.865 Å), letting more space for the heavier Si atom to be occupied inside the hexagonal ring. The interstitial defect could lead to the local melting effect at the lower melting point. This defect formation energy is higher than most of the linear defects, which has a difference of 2.419 eV compared with the linear 8-4 defect

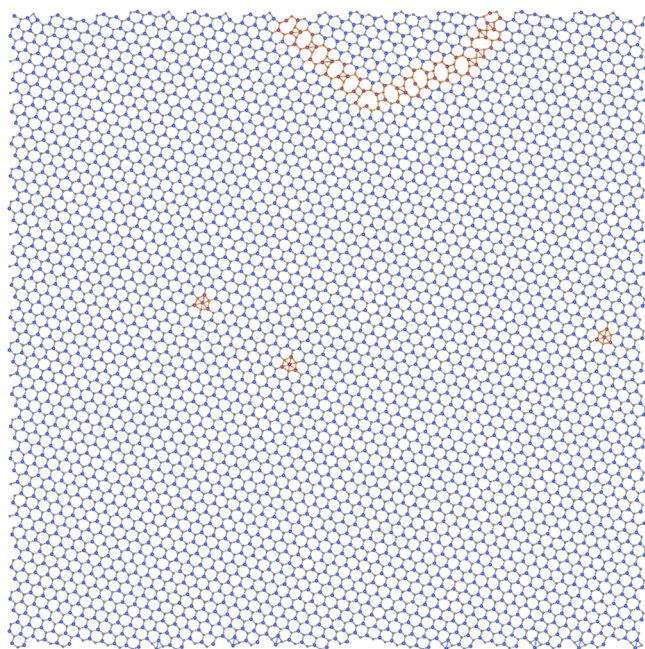case. Figure 6 depicts the SiC monolayer surface structure with the strains highlighted in brown.

Figure 6. Overview of the 2D SiC model relaxed at 300 K using the MD simulation with a system of 6240 Si and C atoms.

In order to understand the influence of defects on the adsorption of hydrogen, an adsorbed hydrogen atom is dropped onto the most easily formed linear defect form (8-4 defect). The obtained results are presented in Table 5 and

Table 5. Adsorption Energy on the SiC Defect Sites (eV)

adsorption site	adsorption energy
T_1	−0.942
T_2	−2.486
T_3	−1.051
T_4	−1.932
T_5	−0.712
T_6	−0.374

Figure 7. The adsorption energy of hydrogen on top position number T_2 gives the lowest value, then T_4, T_3, and finally T_1. All of these adsorption values are more negative than the adsorption values of the pristine lattice (T_5, T_6). This indicates
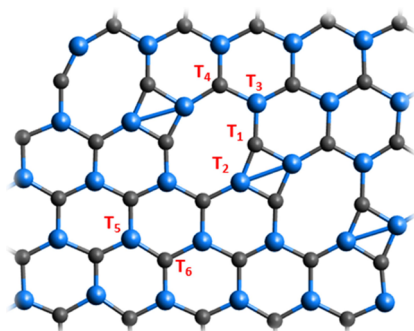

Figure 7. Adsorption sites of hydrogen atoms on linear defect (8-4).

a prediction about the adsorption capacity, and hydrogen atoms adsorb more readily on the defect surface than on the pristine SiC surface.

4. CONCLUSIONS

We calculated the hydrogen adsorption energy on a pristine two-dimensional silicon carbide using the DFT approach. Only two stable adsorption sites have been found, both are on the top of the adsorbent atom (C and Si atom). The most negative hydrogen adsorption energy in consideration of ZPE was found at the T_{Si} configuration. We conclude that the most favorable adsorption site is the T_{Si} site. It agrees well with the vibrational energy calculation, where the hydrogen atom in the T_{Si} configuration has the lowest vibrational energy. Most of the hydrogen vibrational energy comes from the z-axis vibration for all the configurations. The local deformations of 2D SiC caused by H adsorption are also observed. In the T_c configuration, the H atom has caused more distortion compared with the T_{Si} case. The distortion of the adsorbent atom is the most significant along the z-axis for both configurations. At last, we present five defects that could be found in 2D silicon carbide and their formation energies. Those defects are the linear (8-4) defect, the silicon interstitial defect, the divacancy (4-8-8-4) defect, the divacancy (8-4-4-8) defect, and the divacancy (4-10-4) defect. The linear (8-4) defect is verified to have the lowest formation energy and is the most expected defect to be formed. Furthermore, hydrogen atoms adsorb more readily on the defect surface than on the pristine SiC surface. From the results, this study can be an important note in the future for any hydrogen energy application, in which the possibly defects need to be considered in the experiment.

■ AUTHOR INFORMATION

Corresponding Author

Hanh Thi Thu Tran − *Laboratory of Computational Physics, Faculty of Applied Science, Ho Chi Minh City University of Technology (HCMUT), Ho Chi Minh City 70000, Vietnam; Vietnam National University Ho Chi Minh City, Ho Chi Minh City 70000, Vietnam;* ⊙ orcid.org/0000-0002-0841-7682; Email: thuhanhsp@hcmut.edu.vn

Authors

Phi Minh Nguyen − *Laboratory of Computational Physics, Faculty of Applied Science, Ho Chi Minh City University of Technology (HCMUT), Ho Chi Minh City 70000, Vietnam; Vietnam National University Ho Chi Minh City, Ho Chi Minh City 70000, Vietnam*

Hoa Van Nguyen − *Laboratory of Computational Physics, Faculty of Applied Science, Ho Chi Minh City University of Technology (HCMUT), Ho Chi Minh City 70000, Vietnam; Vietnam National University Ho Chi Minh City, Ho Chi Minh City 70000, Vietnam*

Vi Toan Lam − *Laboratory of Computational Physics, Faculty of Applied Science, Ho Chi Minh City University of Technology (HCMUT), Ho Chi Minh City 70000, Vietnam; Vietnam National University Ho Chi Minh City, Ho Chi Minh City 70000, Vietnam*

Tranh Thi Nhu Duong − *Laboratory of Computational Physics, Faculty of Applied Science, Ho Chi Minh City University of Technology (HCMUT), Ho Chi Minh City 70000, Vietnam; Vietnam National University Ho Chi Minh City, Ho Chi Minh City 70000, Vietnam*

Tet Vui Chong − *Faculty of Engineering and Quantity Surveying, INTI International University, Nilai, Negeri Sembilan 71800, Malaysia*

Complete contact information is available at:
https://pubs.acs.org/10.1021/acsomega.2c04532

Author Contributions

H.T.T.T. conceived the idea of developing the research. P.N.M. conducted the simulation. H.T.T.T. and P.M.N. analyzed data, wrote the manuscripts, and collected the most relevant references. All authors contributed to the review of the manuscript and approved the final version of the manuscript.

Notes

The authors declare no competing financial interest.

■ REFERENCES

(1) Geim, A.; Novoselov, K. The Rise Of Graphene. *Nat. Mater.* **2007**, *6*, 183−191.

(2) Thi Thu Hanh, T.; Minh Phi, N.; Van Hoa, N. Hydrogen Adsorption On Two-Dimensional Germanene And Its Structural Defects: An Ab Initio Investigation. *Phys. Chem. Chem. Phys.* **2020**, *22*, 7210−7217.

(3) Sun, L.; Li, Y.; Li, Z.; Li, Q.; Zhou, Z.; Chen, Z.; Yang, J.; Hou, J. Electronic Structures Of Sic Nanoribbons. *J. Chem. Phys.* **2008**, *129*, No. 174114.

(4) Tranh, D.; Hoang, V.; Hanh, T. Modeling Glassy Sic Nanoribbon By Rapidly Cooling From The Liquid: An Affirmation Of Appropriate Potentials. *Phys. B* **2021**, *608*, No. 412746.

(5) Giang, N.; Hanh, T.; Ngoc, L.; Nga, N.; Van Hoang, V. Formation Of Graphene On BN Substrate By Vapor Deposition Method And Size Effects On Its Structure. *Phys. B* **2018**, *534*, 26−33.

(6) Susi, T.; Skákalová, V.; Mittelberger, A.; Kotrusz, P.; Hulman, M.; Pennycook, T.; Mangler, C.; Kotakoski, J.; Meyer, J. Computational Insights And The Observation Of Sic Nanograin Assembly: Towards 2D Silicon Carbide. *Sci. Rep.* **2017**, *7*, 4399.

(7) Khan, F.; Broughton, J. Relaxation Of Icosahedral-Cage Silicon Clusters Via Tight-Binding Molecular Dynamics. *Phys. Rev. B* **1991**, *43*, 11754−11761.

(8) Aufray, B.; Kara, A.; Vizzini, S.; Oughaddou, H.; Léandri, C.; Ealet, B.; Le Lay, G. Graphene-Like Silicon Nanoribbons On Ag(110): A Possible Formation Of Silicene. *Appl. Phys. Lett.* **2010**, *96*, No. 183102.

(9) Vogt, P.; De Padova, P.; Quaresima, C.; Avila, J.; Frantzeskakis, E.; Asensio, M.; Resta, A.; Ealet, B.; Le Lay, G. Silicene: Compelling Experimental Evidence For Graphenelike Two-Dimensional Silicon. *Phys. Rev. Lett.* **2012**, *108*, No. 155501.

(10) Lin, S.; Zhang, S.; Li, X.; Xu, W.; Pi, X.; Liu, X.; Wang, F.; Wu, H.; Chen, H. Quasi-Two-Dimensional Sic And Sic2: Interaction Of Silicon And Carbon At Atomic Thin Lattice Plane. *J. Phys. Chem. C* **2015**, *119*, 19772−19779.

(11) Hsueh, H.; Guo, G.; Louie, S. Excitonic Effects In The Optical Properties Of A Sic Sheet And Nanotubes. *Phys. Rev. B* **2011**, *84*, No. 085404.

(12) Lin, X.; Lin, S.; Xu, Y.; Hakro, A.; Hasan, T.; Zhang, B.; Yu, B.; Luo, J.; Li, E.; Chen, H. Ab Initio Study Of Electronic And Optical Behavior Of Two-Dimensional Silicon Carbide. *J. Mater. Chem. C* **2013**, *1*, 2131.

(13) Feng, Z.; Choyke, W.; Powell, J. Raman Determination Of Layer Stresses And Strains For Heterostructures And Its Application To The Cubic Sic/Si System. *J. Appl. Phys.* **1988**, *64*, 6827−6835.

(14) Gali, A. Ab Initiostudy Of Nitrogen And Boron Substitutional Impurities In Single-Wall Sic Nanotubes. *Phys. Rev. B* **2006**, *73*, No. 245415.

(15) Baumeier, B.; Krüger, P.; Pollmann, J. Structural, Elastic, And Electronic Properties Of Sic, BN, And Beo Nanotubes. *Phys. Rev. B* **2007**, *76*, No. 085407.

(16) Zhao, M.; Xia, Y.; Li, F.; Zhang, R.; Lee, S. Strain Energy And Electronic Structures Of Silicon Carbide Nanotubes: Density Functional Calculations. *Phys. Rev. B* **2005**, *71*, No. 085312.

(17) Plimpton, S. Fast Parallel Algorithms For Short-Range Molecular Dynamics. *J. Comput. Phys.* **1995**, *117*, 1−19.

(18) Vashishta, P.; Kalia, R.; Nakano, A.; Rino, J. Interaction Potential For Silicon Carbide: A Molecular Dynamics Study Of Elastic Constants And Vibrational Density Of States For Crystalline And Amorphous Silicon Carbide. *J. Appl. Phys.* **2007**, *101*, 103515.

(19) Chabi, S.; Guler, Z.; Brearley, A.; Benavidez, A.; Luk, T. The Creation Of True Two-Dimensional Silicon Carbide. *Nanomaterials* **2021**, *11*, 1799.

(20) Freeman, C.; Claeyssens, F.; Allan, N.; Harding, J. Graphitic Nanofilms As Precursors To Wurtzite Films: Theory. *Phys. Rev. Lett.* **2006**, *96*, No. 066102.

(21) Kohn, W.; Sham, L. Self-Consistent Equations Including Exchange And Correlation Effects. *Phys. Rev.* **1965**, *140*, A1133−A1138.

(22) Ordejón, P.; Artacho, E.; Soler, J. Self-Consistent Order-N density-Functional Calculations For Very Large Systems. *Phys. Rev. B* **1996**, *53*, R10441−R10444.

(23) Soler, J.; Artacho, E.; Gale, J.; García, A.; Junquera, J.; Ordejón, P.; Sánchez-Portal, D. The SIESTA Method Forab Initioorder-Nmaterials Simulation. *J. Phys.: Condens. Matter* **2002**, *14*, 2745−2779.

(24) Perdew, J.; Burke, K.; Ernzerhof, M. Generalized Gradient Approximation Made Simple. *Phys. Rev. Lett.* **1996**, *77*, 3865−3868.

(25) Zhang, Y.; Yang, W. Comment On "Generalized Gradient Approximation Made Simple". *Phys. Rev. Lett.* **1998**, *80*, 890−890.

(26) Hoang Giang, N.; Tran, T.; Hoang, V. Structural And Thermodynamic Properties Of Two-Dimensional Confined Germanene: A Molecular Dynamics And DFT Study. *Mater. Res. Express* **2019**, *6*, No. 086411.

(27) Hanh, T.; Takimoto, Y.; Sugino, O. First-Principles Thermodynamic Description Of Hydrogen Electroadsorption On The Pt(111) Surface. *Surf. Sci.* **2014**, *625*, 104−111.

(28) Hanh, T.; Hang, N. A DFT Study Of Hydrogen Electroadsorption On The Missing Row Pt(1 1 0)-(1×2) Surface. *Comput. Mater. Sci.* **2017**, *138*, 295−301.

(29) Hanh, T.; Van Hoa, N. Zero-Point Vibration Of The Adsorbed Hydrogen On The Pt(110) Surface. *Adsorption* **2020**, *26*, 453−459.

(30) Dekock, R. L.; Gray, H. B.*Chemical Structure and Bonding*, 1st ed.; University Science Books: Sausalito, 1989; p 199.

(31) Landau, L.; Lifshitz, E.*Quantum mechanics*; Elsevier Butterworth-Heinemann: Oxford, 1958; p 319.

(32) Ivanovskaya, V.; Zobelli, A.; Teillet-Billy, D.; Rougeau, N.; Sidis, V.; Briddon, P. Hydrogen Adsorption On Graphene: A First Principles Study. *Eur. Phys. J. B* **2010**, *76*, 481−486.

(33) Tomonari, M.; Sugino, O. DFT Calculation Of Vibrational Frequency Of Hydrogen Atoms On Pt Electrodes: Analysis Of The Electric Field Dependence Of The Pt−H Stretching Frequency. *Chem. Phys. Lett.* **2007**, *437*, 170−175.

(34) Hanh, T. The Nature Of The Hydrogen Interaction On The Unreconstructed Platinum (110) Surface: Ab-Initio Study. *Phys. Scr.* **2020**, *96*, No. 025707.

(35) Padilha, J.; Pontes, R. Electronic And Transport Properties Of Structural Defects In Monolayer Germanene: An Ab Initio Investigation. *Solid State Commun.* **2016**, *225*, 38−43.

(36) Qin, H.; Sorkin, V.; Pei, Q.; Liu, Y.; Zhang, Y. Failure In Two-Dimensional Materials: Defect Sensitivity And Failure Criteria. *J. Appl. Mech.* **2020**, *87*, 1−32.

(37) Bhatt, M.; Kim, H.; Kim, G. Various Defects In Graphene: A Review. *RSC Adv.* **2022**, *12*, 21520−21547.

(38) Kyushin, S.; Kurosaki, Y.; Otsuka, K.; Imai, H.; Ishida, S.; Kyomen, T.; Hanaya, M.; Matsumoto, H. Silicon−Silicon Π Single Bond. *Nat. Commun.* **2020**, *11*, 4009.

(39) Nørskov, J.; Bligaard, T.; Logadottir, A.; Kitchin, J.; Chen, J.; Pandelov, S.; Stimming, U. Trends In The Exchange Current For Hydrogen Evolution. *J. Electrochem. Soc.* **2005**, *152*, J23.

(40) Hinnemann, B.; Moses, P.; Bonde, J.; Jørgensen, K.; Nielsen, J.; Horch, S.; Chorkendorff, I.; Nørskov, J. Biomimetic Hydrogen Evolution: Mos2 Nanoparticles As Catalyst For Hydrogen Evolution. *J. Am. Chem. Soc.* **2005**, *127*, 5308−5309.

(41) Ling, C.; Shi, L.; Ouyang, Y.; Chen, Q.; Wang, J. Transition Metal-Promoted V 2 CO 2 (Mxenes): A New And Highly Active Catalyst For Hydrogen Evolution Reaction. *Adv. Sci.* **2016**, *3*, No. 1600180.

(42) Thomas, A.*NIST-JANAF Thermochemical Tables - SRD 13*; National Institute of Standards and Technology, 2013.